The Role of Midtropospheric Winds in the Evolution and Maintenance of Low-Level Mesocyclones

HAROLD E. BROOKS AND CHARLES A. DOSWELL III

NOAA/National Severe Storms Laboratory, Norman, Oklahoma

ROBERT B. WILHELMSON

Department of Atmospheric Sciences, University of Illinois, Urbana, Illinois

(Manuscript received 5 April 1993, in final form 2 August 1993)

ABSTRACT

Using a three-dimensional numerical model, supercell simulations initialized in environments characterized by hodographs with large curvature in the lowest 3 km and a range of linear midlevel shears are investigated. For low values of the midlevel shear (0.005 s^{-1}), the storm develops a mesocyclone at the lowest model level within the first hour of the simulation. The gust front starts to move ahead of the main updraft and cuts off the inflow to the storm by approximately 2 h, resulting in decay of the initial storm and growth of a new rotating storm on the outflow. As the midlevel shear increases to approximately 0.010 s^{-1}, the initial development of the low-level mesocyclone is delayed, but the mesocyclone that develops is more persistent, lasting for over 2 h. Further increases of the shear to 0.015 s^{-1} result in the suppression of any low-level mesocyclone, despite the presence of intense rotation at midlevels of the storm.

We hypothesize that differences in the distribution of precipitation within the storms, resulting from the changes in storm-relative winds, are responsible for the changes in low-level mesocyclone development. In the weak-shear regime, storm-relative midlevel winds are weak and much of the rain is carried by the midlevel mesocyclonic flow to fall west of the updraft. As this rain evaporates, baroclinic generation of vorticity in the downdraft leads to mesocyclogenesis at low levels of the storm. The outflow from the cold air associated with the rain eventually undercuts the inflow to the storm. As the midlevel shear increases, the storm-relative winds increase and more of the rain generated by the storm falls well away from the updraft. As a result, baroclinic generation of vorticity in the downdraft immediately west of the updraft is slower. Once a low-level mesocyclone is generated, however, the weaker outflow allows the mesocyclone to persist.

1. Introduction

Supercell thunderstorms represent an important problem in the severe weather warning process for operational meteorologists. Supercells are characterized by a region of persistent rotation known as a mesocyclone that extends through most of the depth of the thunderstorm. They also have intense updrafts, typically move to the right of the vertically integrated mean environmental wind, and may persist for hours rather than a few tens of minutes as ordinary thunderstorms do. As a result, they often produce long swaths of severe weather. This last point makes them a particularly important forecast problem for the public. The WSR-88D radars being installed in a network around the United States as part of the modernization of the National Weather Service (NWS) take advantage of the existence of rotation at midlevels (~3–7 km) of these storms to observe and identify them.

In experiments at the National Severe Storms Laboratory (NSSL), it has been found that almost all mesocyclonic storms produce some kind of severe weather (large hail, strong straight-line winds, or tornadoes), half produce tornadoes, and almost all strong or violent tornadoes are associated with mesocyclones (Burgess and Lemon 1990). The association of tornadoes with observed mesocyclones makes it possible to use the observation of mesocyclones as part of the tornado warning process with a high probability of detection. However, since only half of all mesocyclones produce tornadoes, overreliance on midlevel mesocyclone identification as a tornado warning criterion could result in an unacceptably high false-alarm rate. Brooks et al. (1993) show examples of what are referred to as "failure modes," in which storms with midlevel mesocyclones fail to produce long-lived *low-level* mesocyclones and, hence, would be unlikely to produce significant tornadoes. In this paper, we explore the connection between the midlevel mesocyclone and low-level mesocyclone and provide a simple conceptual model of processes linking the two.

Corresponding author address: Dr. Harold E. Brooks, NOAA/NSSL, 1313 Halley Circle, Norman, OK 73069.

Theoretical work has been carried out over the last decade to look at the separate issues of the development and maintenance of midlevel and low-level rotation. Davies-Jones (1984) and Rotunno and Klemp (1985) discussed the origin of rotation in midlevels of supercell thunderstorms as the result of tilting the initially horizontal vorticity resulting from vertical wind shear in the thunderstorm environment. Rotunno and Klemp (1985) demonstrated that the origin of the low-level mesocyclone (near the ground) depends on baroclinic processes resulting from the evaporation of rain. Davies-Jones and Brooks (1993) extended this argument to show that tilting of baroclinically generated horizontal vorticity within the rear-flank downdraft could produce positive vertical vorticity within the downdraft. As a result, air reaching the ground within the downdraft could have positive vertical vorticity *before* it encounters the updraft.

A measure of the likelihood that an environment will support thunderstorm rotation at midlevels is the environmental storm-relative helicity $\mathscr{H}$ defined by

$$\mathscr{H}(\mathbf{c}) = -\int_0^h \mathbf{k}\cdot(\mathbf{V}-\mathbf{c})\times\frac{\partial\mathbf{V}}{\partial z}\,dz, \qquad (1)$$

where h is an assumed inflow depth, $\mathbf{c}$ is the storm-motion vector, $\mathbf{V}(z)$ is the environmental wind profile, and $\mathbf{k}$ is the unit vector in the vertical (Davies-Jones et al. 1990). Assuming that long-lived convection occurs, storms are more likely to rotate in high-helicity environments. Helicity has been shown to be a good predictor of the correlation between vertical velocity and vorticity in numerically simulated thunderstorms (Droegemeier et al. 1993).

The development of parameters that directly forecast the likelihood of low-level rotation in an environment has proven more problematic. While the importance of low-level hodograph curvature in discriminating between tornadic and nontornadic environments has been noted in observational studies (e.g., Patrick and Keck 1987; Davies-Jones et al. 1990), it seems that the primary relevance is in the development of midlevel rotation and, hence, supercells. In this paper, we will look at the variety of behaviors seen in low levels of numerically modeled supercells, all originating in high-helicity environments. Earlier numerical studies by Weisman and Klemp (1984) have shown a delay in the development and an increase in the magnitude of low-level vorticity as the shear increases with hodographs that made a semicircle over the lowest 5 km. Weisman and Klemp offer no physical mechanism to explain this behavior.

Our work builds upon the theoretical explanation of low-level mesocyclogenesis of Davies-Jones and Brooks (1993). As a result, we are interested in the location and magnitude of cold air generated in downdrafts. The source of the cold air is evaporation of precipitation. Therefore, we will focus on the distribution of precipitation around supercells and the subsequent generation of cold air by evaporation.[1]

In particular, we are interested in the effects of midtropospheric, environmental winds on precipitation and low-level mesocyclogenesis in simulated storms. Two important effects of the midlevel winds are possible: changes in the precipitation distribution and changes in the storm motion. The latter affects the helicity of the inflow air entering the storm, which, in turn, affects the midlevel structure of the storm. The change in precipitation distribution leads to changes at low levels in the location of cold air resulting from evaporation of precipitation. Thus, we hypothesize that midlevel winds, and hence, midlevel shear, play an important role in the *low-level* vorticity structure of a supercell thunderstorm, even though the vorticity associated with environmental shear in midlevels may not be tilted into the low-level flow. To look at the effects of midlevel shear on low-level supercell structure, we have carried out a series of numerical supercell thunderstorm simulations in which the magnitude of the 3–7-km shear has been varied, with all other parameters of the background initial state held constant between the simulations.

2. Experiment description

The numerical model used to generate the simulations is that of Klemp and Wilhelmson (1978), as modified by Wilhelmson and Chen (1982), to which the reader is referred for details of the computational scheme. It is three-dimensional, fully compressible, and uses a Kessler microphysical parameterization. The domain is 70 km × 70 km × 16 km, with 1-km horizontal grid spacing and a vertical grid increment that varies as a hyperbolic tangent function of height from 200 m near the ground to 600 m near the top. The horizontal grid spacing is too large to resolve the tornadic circulation itself but is sufficient for resolving large mesocyclonic circulations. The Coriolis effect and surface drag are excluded for simplicity, while a Rayleigh damping layer was included in the stratosphere (above 12 km) to limit gravity waves at the top of the model. Each simulation was carried out until at least 9000 s, with a large time step of 5 s. Storms are initialized with a warm thermodynamic "bubble" with a horizontal semiaxis of 10 km and a vertical semiaxis of 1.4 km. The bubble is centered at the 1.4-km altitude and has a maximum temperature perturbation of 2 K.

All of the simulations have the same thermodynamic profile (Fig. 1). The sounding is similar to, but drier

[1] While the observational studies have focused on the questions about tornadoes, we will be looking at the questions about low-level mesocyclones. Not all low-level mesocyclones produce tornadoes but computational restrictions make it impossible for us to resolve tornadoes within the numerical model in a way that allows us to carry out a large number of simulations economically.

above the boundary layer than, that used by Weisman and Klemp (1982, 1984). The surface moisture is 15 g kg^{-1} decreasing to 14 g kg^{-1} at 1 km, resulting in a convective available potential energy (CAPE) of about 2100 J kg^{-1}. The hodograph for the lowest 3 km of the atmosphere is characterized by a rapid veering of the shear vector (Fig. 2). Above 3 km, the v component of the environmental wind at the initial time is held constant at 15 m s^{-1}. Shear above 3 km is confined to the u component, with $u = 0$ m s^{-1} at 3 km, increasing linearly to 7 km. The 3–7-km shear is varied in the experiments from 0.005 to 0.015 s^{-1} in increments of 0.001 s^{-1}, resulting in a range of u between 20 and 60 m s^{-1} at 7 km. The range of shears chosen spans the values of midlevel shear typically associated with supercells (e.g., Marwitz 1972; Fujita et al. 1970), although the 0.015 s^{-1} case may be stronger than that usually observed. The environmental wind above 7 km at the initial time is held constant at the 7-km value. Although we can vary the shear directly, the helicity is a function of the storm motion, so its value cannot be known a priori. After the completion of the simulation, the helicity as a function of time can be computed. For the mature stage of the supercells in this study, the range of helicity is 517–772 J kg^{-1}, well into the range associated with strongly rotating storms (Davies-Jones et al. 1990). The magnitude of the storm-relative 7-km winds vary from 13.4 to 40.2 m s^{-1} during the mature phase of the storms (Fig. 2).

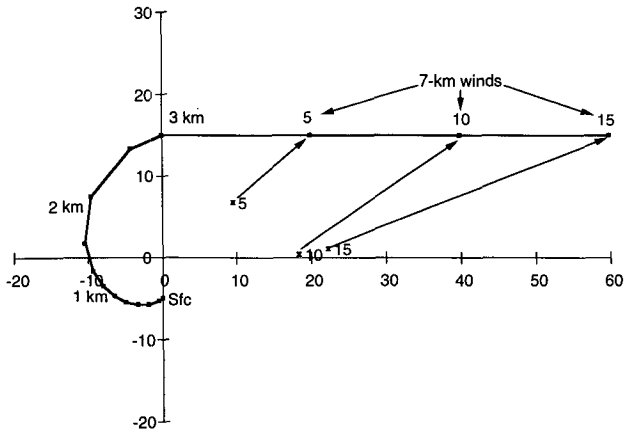

FIG. 2. Hodographs and storm motion, indicated by asterisk for each case, from 3600 to 7200 s. The location of the 7-km winds on the hodograph and the storm-relative wind vector at 7 km are shown for each case. Axes are in meters per second. Numbers on storm motion and 7-km winds indicate 1000 × shear.

3. Results

For all but the weakest midlevel shear case, a single long-lived updraft dominates each simulation. In the weakest midlevel shear case, a secondary updraft rapidly develops on the initial storm gust front, at approximately 2 h from initiation, after cold outflow air has undercut the initial updraft. As the first updraft dies, the second updraft intensifies and persists.

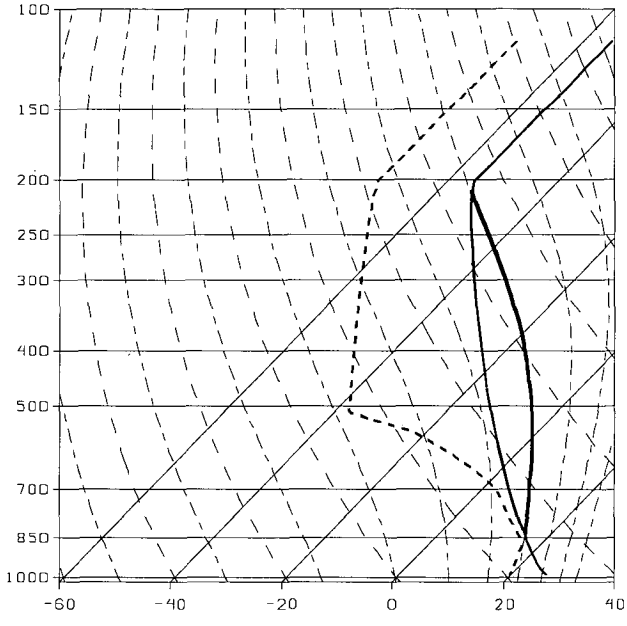

FIG. 1. Thermodynamic profile used in soundings. Solid line is temperature, and dashed line is dewpoint. Heavy line indicates moist adiabat associated with parcel ascent.

All of the storms develop midlevel mesocyclones (defined by having vorticity greater than 0.01 s^{-1}) by approximately 1800 s into the simulations (Fig. 3). The midlevel rotation persists through the end of the simulations. The simulated production of midlevel mesocyclones is consistent with the notion that the high helicity values of the environmental hodographs should support supercell thunderstorm development. Of most interest to us, however, is the development and persistence of the low-level mesocyclone.

a. Initiation of low-level mesocyclones

To focus the discussion of low-level mesocyclogenesis, we will look at only three of the simulated storms—those initiated with 3–7-km shears S of 0.005, 0.010, and 0.015 s^{-1}. As the midlevel shear increases, the time to develop significant vorticity at low levels increases (Fig. 3). Low-level vorticity ζ in the $S = 0.015$ s^{-1} case barely reaches $\zeta = 0.005$ s^{-1} during the simulation. Until 9000 s, there is no vorticity of mesocyclonic values in the lowest 2 km and that which appears by 9000 s occurs outside the region of interest on the edge of the model domain. In the $S = 0.005$ s^{-1} case, on the other hand, the peak low-level vorticity rapidly increases to well over $\zeta = 0.01$ s^{-1} approximately half an hour after the initial vorticity maximum at midlevels. Generation of vorticity at low levels is slower in the $S = 0.010$ s^{-1} case, taking approximately an hour for a low-level mesocyclone to develop after the midlevel mesocyclone is seen.

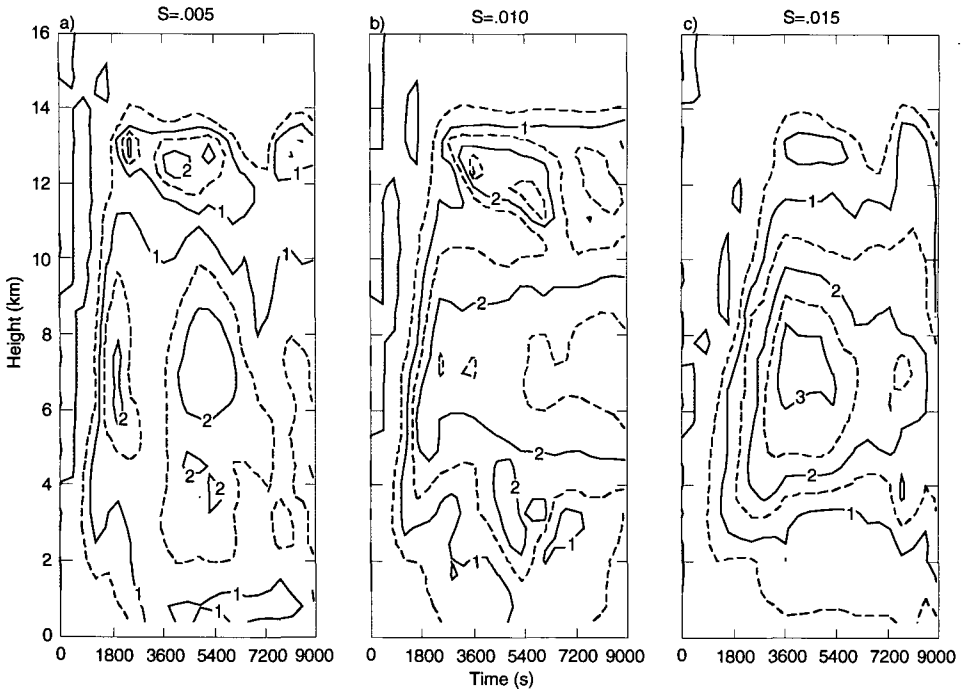

FIG. 3. Time–height cross sections of the maximum vertical vorticity in the first 9000 s of the simulations. The contour interval is 0.005 s^{-1}, and every other contour line is dashed. Labels on selected contour lines are multiplied by 100, so that a label of 1 indicates $\zeta = 0.010\ s^{-1}$: (a) $S = 0.005\ s^{-1}$, (b) $S = 0.010\ s^{-1}$, and (c) $S = 0.015\ s^{-1}$.

The distribution of precipitation and the associated evaporation is the critical factor in understanding the development of the low-level vorticity in these storms. As discussed by Davies-Jones and Brooks (1993), development of vertical vorticity due to baroclinic generation of horizontal vorticity in the evaporatively cooled air in the rear-flank downdraft and subsequent tilting within the downdraft is a significant factor in the development of low-level mesocyclones. A comparison of the midlevel and low-level rainwater fields with the updraft location in the low and high midlevel shear cases reveals that one of the effects of the strong storm-relative winds in the high-shear case is to blow rain away from the updraft (Fig. 4). Even though a significant amount of rain is found near the updraft at 5.1 km in both cases, at the lowest model level, rain in the high-shear case is separated from the updraft. This point is further emphasized by considering the distribution of rain at the lowest model level as a function of distance from the midlevel updraft (Fig. 5). Though the onset of precipitation occurs at approximately the same time in both cases, heavy precipitation in the vicinity of the updraft begins earlier and falls closer to the updraft in the low-shear case. In that simulation, rain at midlevels remains close to the updraft as it falls and the mesocyclonic circulation tends to pull the rain around the updraft to the west and southwest of the updraft. With substantial precipitation falling near the updraft, baroclinic generation of vorticity at low levels is much greater in the low-shear case than in the high-shear case. The middle-shear case falls in between these two extremes, with less precipitation in the vicinity of the updraft than in the low-shear case but more than in the high-shear case. It is important to note that the relevant physical parameter in the flow is the *magnitude of the storm-relative winds,* not the magnitude of the shear.

The character of the low-level flow in the high-shear case is best illustrated by looking at the relationship of the velocity, rainwater, and perturbation temperature fields. The gust front trails off to the southwest of the updraft, and the velocity field is weak. The strongest temperature gradients associated with the rainwater are well to the southwest of the updraft, and vorticity is small at 3600 s, with a peak value of $\zeta = 0.0017\ s^{-1}$ (Fig. 6a). The velocity field is also perpendicular to the temperature gradient for the most part. As time goes on (Fig. 6b), the temperature gradient remains small in the vicinity of the updraft and any flow parallel to the temperature gradient is away from the updraft. As a result, vorticity is still small and there is no hint of an organized circulation at low levels, even though there is a suggestion of a hook echo in the rainwater field.

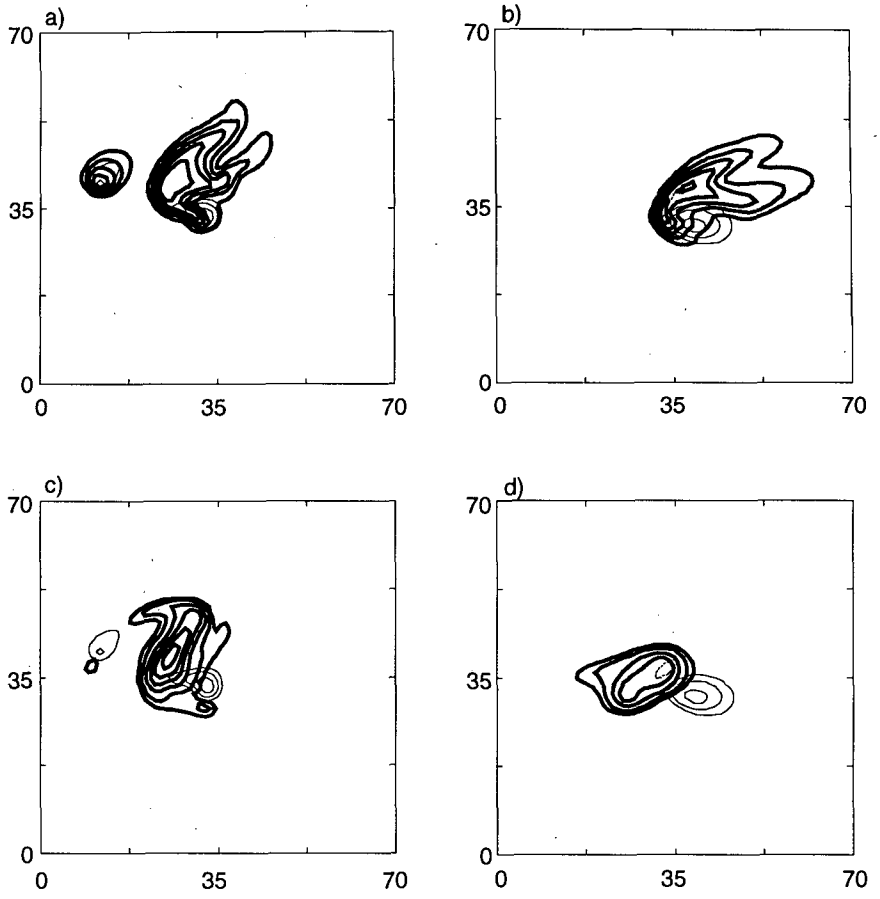

FIG. 4. At 3600 s, updraft at 5.1 km and (a) rainwater at 5.1 km in $S = 0.005\ s^{-1}$ case, (b) rainwater at 5.1 km in $S = 0.015\ s^{-1}$ case, (c) rainwater at 0.1 km in $S = 0.005\ s^{-1}$ case, and (d) rainwater at 0.1 km in $S = 0.015\ s^{-1}$ case. Rainwater is indicated by heavy contours with interval 2 g kg^{-1} with a minimum contour of 0.5 g kg^{-1}. The vertical velocity contour is 10 m s^{-1}. The axes are labeled in kilometers, with (0, 0) the southwest corner of the domain.

b. Persistence of low-level mesocyclones

Although the low-shear case is the first to develop a large value of vertical vorticity at low levels, the *duration* of this high vorticity is brief (Fig. 3), as the outflow from the precipitation that has fallen to the west and southwest of the main updraft is carried toward the east around the mesocyclone. The high vorticity forms, as expected, along the strong temperature gradient associated with the outflow from the precipitation where the flow is parallel to the temperature gradient (Fig. 7a). The region of the vorticity maximum slides to the south of the outflow and decays rapidly, leaving a region of small vorticity to the southeast of the hook in the precipitation field. A new center of low-level vorticity then forms on the *north* side of the surging outflow in the same region relative to the precipitation as the first vorticity center (Fig. 7b). This vorticity maximum is relatively shallow and short-lived (Fig. 3). As the storm continues to develop, only a little precipitation falls to the north and east of the updraft and the updraft is embedded in precipitation similar to the observed character of a high-precipitation (HP) supercell (Moller et al. 1990). The second vorticity maximum moves anticyclonically around the main body of the precipitation region, while a third vorticity region develops on the northeast side of the precipitation. Again, this vorticity maximum is shallow, with mesocyclonic vorticity values confined to the lowest model level.

The low-level mesocyclone in the middle-shear case, although slower to develop than in the low-shear case, is remarkably persistent.[2] Once the low-level mesocy-

[2] By approximately 13 800 s, an unphysical updraft generated along the domain boundary becomes significant. As a result, the simulation was repeated with a larger domain (96 km × 96 km) out to 18 000 s, with the time step reduced to 3 s after 12 000 s of simulation time. Although the simulations are not identical, apparently due to different translation speeds of the computational domain, they are very similar. A second low-level vorticity region forms at approximately 14 400 s,

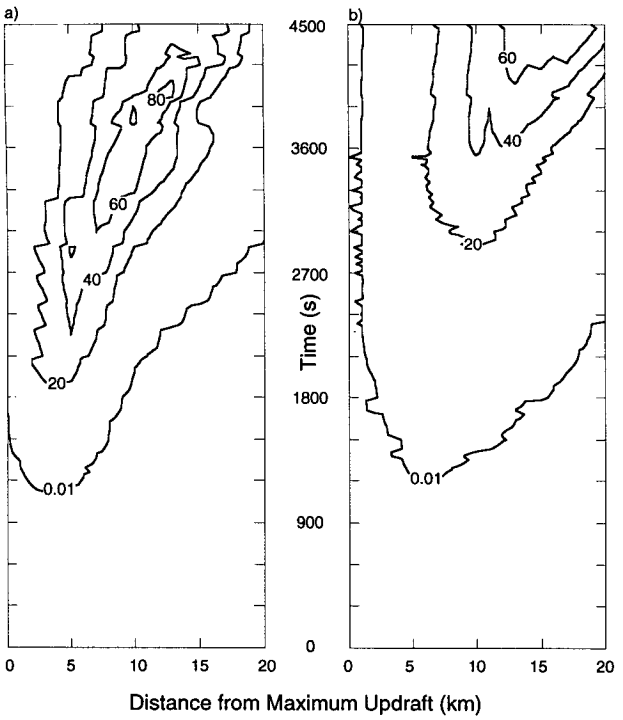

FIG. 5. Rainwater (g kg^{-1}) at 0.1 km as a function of horizontal distance from the location of the updraft at 5.1 km in first 4500 s for (a) $S = 0.005$ s^{-1} and (b) $S = 0.015$ s^{-1}. Values are obtained by summing point values of rainwater around equal radius circles centered on the updraft.

clone is established, the maximum vorticity is greater than 0.01 s^{-1} throughout the entire depth of the troposphere with the exception of a brief period near 7200 s at 2–2.5 km in altitude. In contrast to the $S = 0.005$ s^{-1} case, the persistent nature of the high vorticity at low levels is apparent (Fig. 8). Vorticity greater than 0.015 s^{-1} extends from the surface to 10 km for a significant period of time. Animations reveal that while the shape of the region changes through time, it is clear that the region of high vorticity is continuous in time, in direct contrast to the low-shear case. Again, the distribution of precipitation is critical in the evolution of the mesocyclone. The lesser amount of rain in the vicinity of the main updraft (Fig. 9), in comparison to the low-shear case, causes the low-level mesocyclone to develop more slowly and also produces weaker outflow than in the low-shear case. The weaker outflow allows the mesocyclone to persist for a much longer period of time.

Within the low-level mesocyclone, however, there are features of interest in the temporal evolution. By following the evolution of the flow, this becomes apparent. In the early stages of development, vorticity is not very high, flow behind the gust front is entirely northerly, and the gust front extends south from the main updraft (Fig. 9a). As the low-level mesocyclone intensifies, the gust front moves eastward relative to the updraft, with the associated flow behind the gust front becoming westerly. As a result, the flow centered on the gradient between the updraft and downdraft has become nearly circular (Fig. 9b). The occlusion process continues with the updraft and downdraft wrapping around each other and the mesocyclone increases in size (Fig. 9c). As the gust front continues to move eastward, the mesocyclone becomes more elongated, stretching out along the gust front (Fig. 9d), until it is aligned nearly due east from the weakening low-level

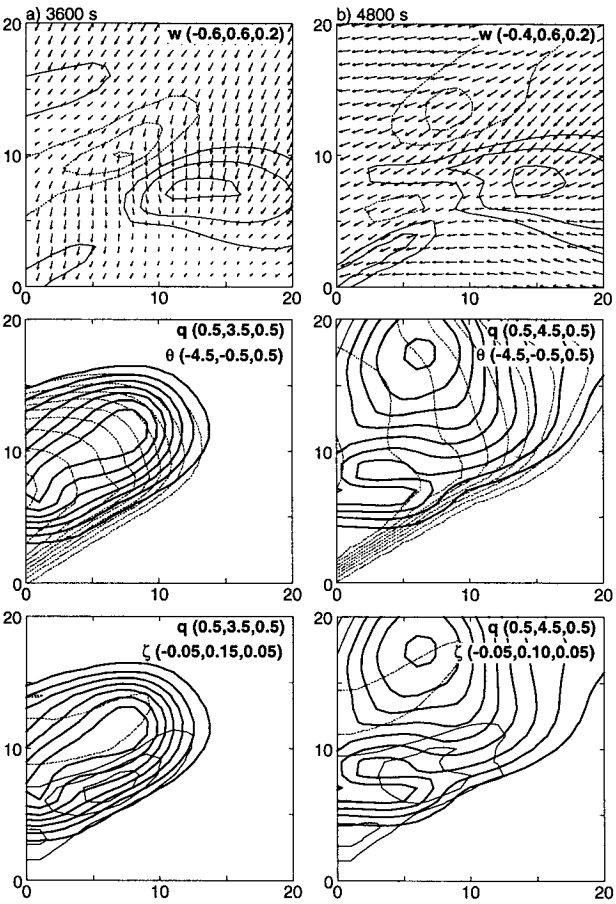

FIG. 6. Horizontal cross sections of 20-km × 20-km portion of domain at 0.1 km in high-shear case. Figures in parentheses give minimum contour value, maximum contour value, and contour interval: vertical velocity w and horizontal storm-relative velocity field (vectors with one grid interval length equal to 20 m s^{-1}) (top panel), rainwater q (heavy line), and perturbation temperature θ (middle), and rainwater and vertical vorticity ζ (light line with contours multiplied by 100) (bottom). Zero contour is suppressed in all cases. Axes are labeled in kilometers from an arbitrary origin: (a) 3600; (b) 4800 s.

and the updraft is still approximately 20 m s^{-1} at 18 000 s. Some issues raised in the large-domain simulation, particularly the repeated development and intensification of submesocyclone-scale vortices, are beyond the scope of this paper and require further investigation.

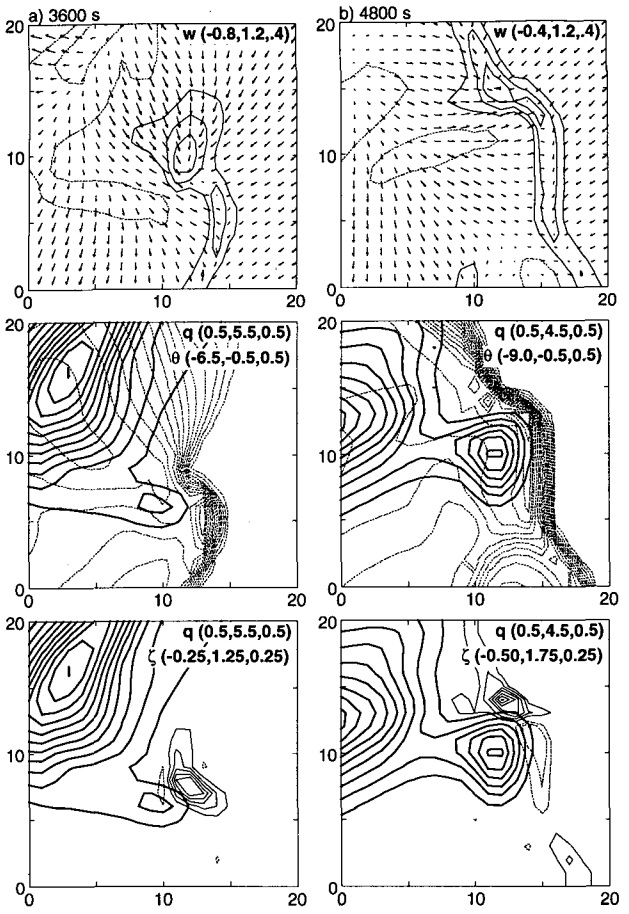

FIG. 7. Same as Fig. 6 except for the low-shear case.

updraft (Fig. 9e). Finally, the flow near the updraft reorganizes as the updraft reintensifies (Fig. 9f). The time between the original intensification and this second peak is approximately an hour. The timing of the cycle of intensification and decay of submesocyclone maxima is similar to that reported by Burgess and Lemon (1990) for cyclic tornadogenesis. It is of interest to note that the maxima in the time history of the vorticity do not necessarily correspond to the most well developed low-level mesocyclones. For instance, the second submesocyclone shown in Fig. 9f (at 10 200 s) is seen at a time when the low-level vorticity is at a relative minimum (Fig. 8). Since high vorticity can occur in regions of large shear along a gust front as well as in the well-developed circulations of the mesocyclone, vorticity is not necessarily the only measure of the character of the mesocyclone.

4. Discussion

The behavior of the modeled storms supports a simple conceptual model of the role of midlevel winds in the development and maintenance of low-level mesocyclones in supercells. The distribution of precipitation in the vicinity of the storm holds the key to understanding the effect of the midlevel winds. Two fundamental processes act to distribute rainwater in the horizontal in the storms. The first is the environmental, storm-relative winds in the vicinity of the storm, which act to blow precipitation away from the updraft. The second is the flow associated with the mesocyclone, the intensity of which is a function of the *low-level* wind field, which wraps precipitation around the updraft. As discussed by Davies-Jones and Brooks (1993), in the model the presence of evaporating precipitation near the updraft in the rear-flank downdraft is essential to the development of low-level mesocyclones. Hence, if the midlevel winds are too strong with respect to the midlevel mesocyclone intensity, little precipitation falls near the updraft and no low-level mesocyclone forms (i.e., the $S = 0.015\ s^{-1}$ case in this paper). If, on the other hand, the midlevel storm-relative winds are weak, a large amount of precipitation falls in the vicinity of the updraft. Hence, development of a low-level mesocyclone is rapid, since evaporation and baroclinic vorticity generation are large. However, the strength of the outflow associated with the cold air can undercut the updraft and cut short the lifetime of the low-level mesocyclone (i.e., the $S = 0.005\ s^{-1}$ case).

This simple model suggests that the development of a long-lived, low-level mesocyclone requires a qualitative balance between the strength of the midlevel

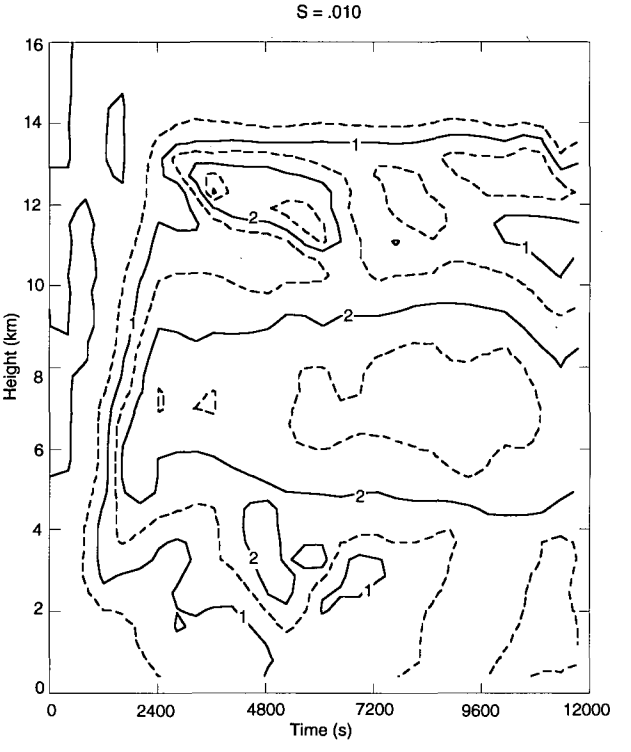

FIG. 8. Same as in Fig. 3 except for the first 12 000 s in $S = 0.010\ s^{-1}$ case.

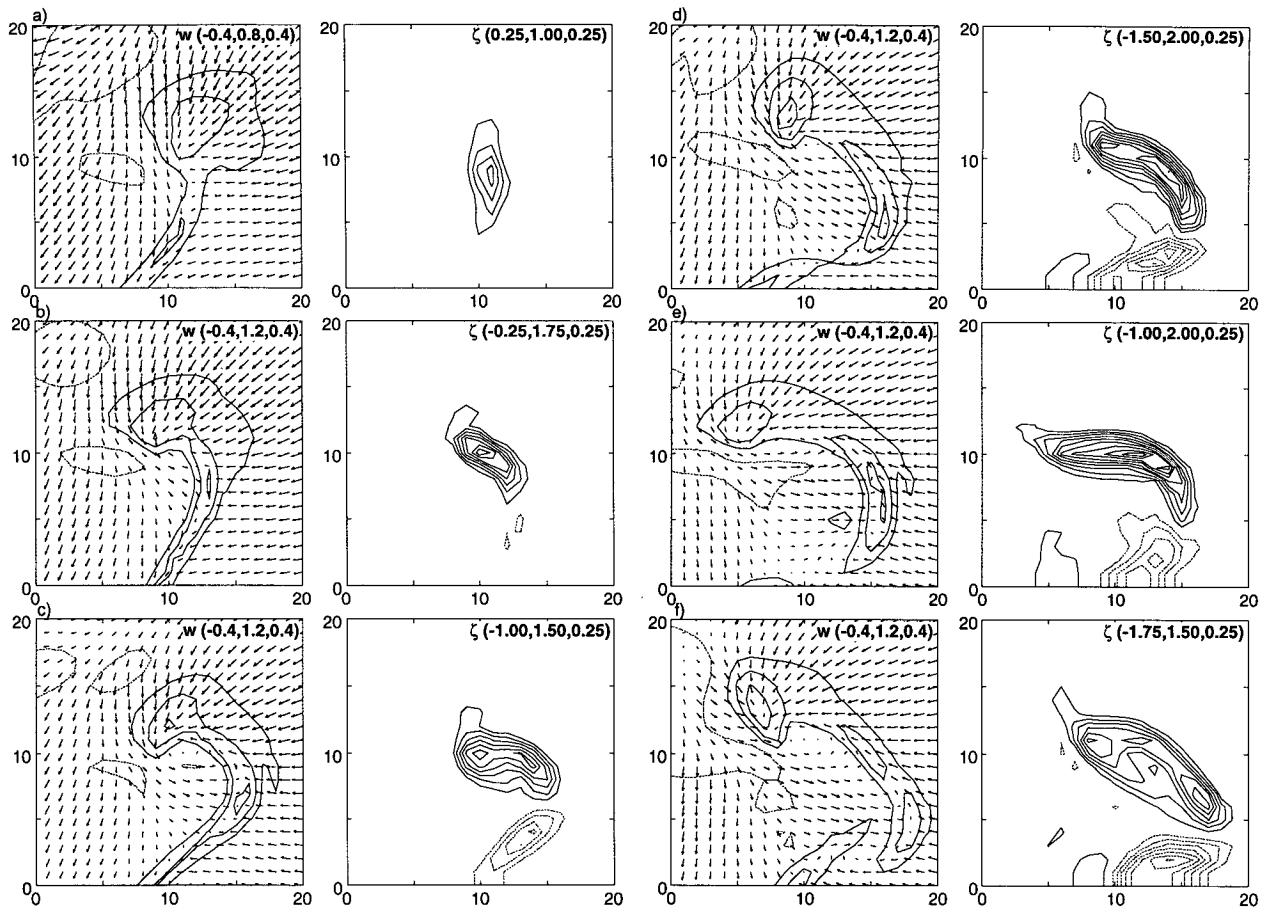

FIG. 9. Evolution of flow field at 0.1 km in $S = 0.010\ s^{-1}$ case. Figures in parentheses give minimum contour value, maximum contour value, and contour interval. Left panel is vertical velocity (contour interval 0.4 m s^{-1}) and horizontal velocity (one grid length equal to 20 m s^{-1}). Right panel is vertical vorticity (contours multiplied by 100). Zero contour is suppressed. Axes are labeled in kilometers from an arbitrary origin: (a) 4200 s, (b) 5400 s, (c) 6600 s, (d) 7800 s, (e) 9000 s, and (f) 10 200 s.

mesocyclone and the midlevel storm-relative winds. Since the midlevel mesocyclone is a product of processes associated with the *low-level* wind profile, this implies that the details of the winds through a large depth of the atmosphere are important in the generation of low-level mesocyclones and, hence, supercell tornadoes. Forecasting techniques that deal only with the low-level wind field of the environment, such as storm-relative environmental helicity (Davies-Jones et al. 1990) or low-level shear magnitude (Rasmussen and Wilhelmson 1983), are essentially forecasting *supercells,* not *tornadoes.* Effective operational tornado forecasting requires the consideration of a deep layer of the environment. Extremely long-lived, low-level mesocyclones, which would be associated with long-track tornadoes or multiple tornadoes from a single storm, will be found in environments with high helicity and strong storm-relative midlevel winds, as illustrated by observations from 12 April 1965, 4 April 1974, and 26 April 1991 (Fig. 10). An interesting secondary result is that such storms may occur in conditions that lead to a long lag between the development of the midlevel mesocyclone and low-level mesocyclone.[3] The similarity of the low-shear case (in which long-lived, low-level rotation was absent) to HP supercells is another interesting feature. Moller et al. (1990) noted that strong and violent tornadoes are not as common in HP supercells and that the hodographs in the two cases they show both have weak storm-relative, midlevel winds. We note, however, that their two cases were in lower-helicity environments ($\leq$300 J kg^{-1}) than we have simulated. As a result, it is premature to assert that the lack of strong tornadoes in HP supercells, as described by Moller et al. (1990), is related to the intensity of the midlevel winds based upon the simula-

[3] In this regard, we note that the significant rotation at low levels in the supercell that produced the long-track Red Rock, Oklahoma, tornado of 26 April 1991 and produced tornadoes for approximately 4 h was first seen approximately an hour after significant midlevel rotation developed (Burgess and Magsig 1993).

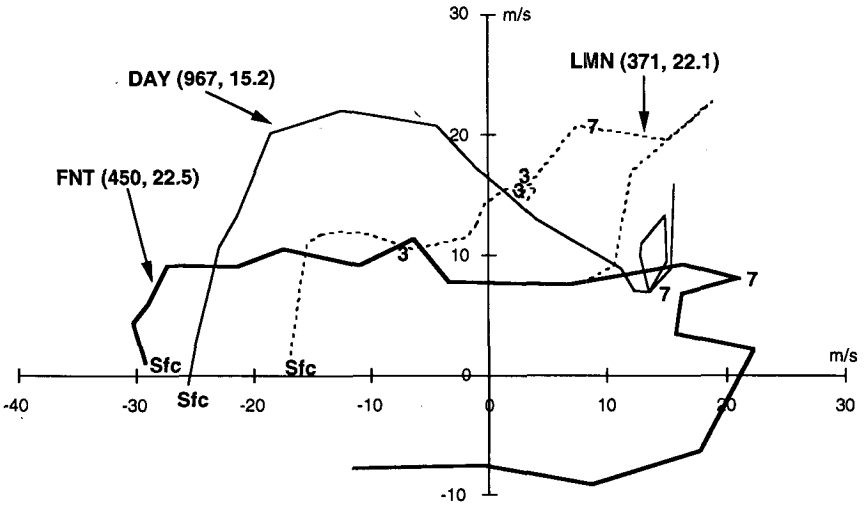

FIG. 10. Storm-relative hodographs associated with long-track, multiple-tornado-producing storms. FNT is from the Flint, Michigan, sounding at 0000 UTC 12 April 1965 (Palm Sunday outbreak), DAY is from the Dayton, Ohio, sounding at 0000 UTC 4 April 1974 (jumbo outbreak), and LMN is from the Lamont, Oklahoma, wind profiler at 2200 UTC 26 April 1991 (Wichita–Andover outbreak). The 3- and 7-km levels are indicated. Figures in parentheses give 0–3-km helicity and 7-km storm-relative wind magnitude.

tions here, but such a possibility needs further exploration.

While the microphysical parameterization in the numerical model used to generate these storms did not include ice-phase processes, this does not seem to be a crucial limitation on the qualitative results. The conceptual model is based primarily on the determination of where and how intense the region of cold air in the vicinity of the updraft is. The critical step related to the microphysics is the cooling of downdraft air by change of phase. Thus, whether that change is from liquid to vapor or solid to liquid to vapor would not seem necessarily to be qualitatively important in determining downdraft intensity, although it might have quantitative importance. Since the fall speed of frozen hydrometeors is different than liquid hydrometeors, it is possible, however, that the presence of ice could affect the *location* as well as the strength of the downdrafts, and since the system is highly nonlinear, it is possible that in some marginal cases ice-phase microphysics might be critical. As implied earlier, a greater limitation on the interpretation may be that all of the simulations we have carried out here have been in high-helicity environments. It is possible that the nature of the balance between the midlevel mesocyclone and midlevel winds is different in environments with low and moderate helicity. The conceptual model implies that a "balanced" state could exist with less helicity, generating a weaker midlevel mesocyclone and weaker storm-relative winds than we have used in our simulations here.

Further, to date we have not explored the potentially significant role the conceptual model assigns to the thermodynamic structure of the environment. To isolate the role of the winds, we have kept the initial temperature and moisture profiles the same in all the simulations. This does not mean that storm behavior is independent of the thermodynamics. In particular, the amount of low-level absolute humidity will help determine the amount of rain produced by the storm, and the relative humidity of the lower and middle troposphere will determine the evaporation. As a result, the magnitude of the cold downdraft air will depend on the vertical distribution of water vapor throughout the depth of the storm. We reemphasize that the critical point of the model is to consider the location and magnitude of evaporatively cooled downdraft air. Thus, thermodynamic considerations do not limit the applicability of our proposed model to the environmental sounding modeled here. Clearly, however, since the moisture profile is critical in determining the amount of precipitation and evaporation in a storm, the thermodynamic structure of the environment offers a rich area for new research and possible application in operational forecasting.

The conceptual model presented here may begin to tie together some threads that have been moving somewhat independently concerning tornado research for many years. Results from earlier numerical simulations of supercells can be understood in the context of the model. The delay in onset and increase in magnitude of high vorticity with increasing shear in the simulations of Weisman and Klemp (1984) are consistent with the increasing midlevel winds in their stronger shear cases. Three of the four supercells shown by Droegemeier et al. (1993) are in environments with

helicity values of approximately 300 J kg^{-1}. The maximum low-level vorticity generated in those storms increased as the storm-relative wind magnitude above 4 km increased from approximately 6.5 to 13 m s^{-1}.

Observationally, most early work on the environments around supercell thunderstorms and tornadoes stressed the need for strong mid- and upper-level winds (e.g., Fawbush et al. 1951; Shuman and Carstensen 1952; Fawbush and Miller 1952, 1954). This resulted in theoretical arguments that attempted to tilt vertical vorticity near the top of thunderstorms down to form tornadoes (e.g., Wegener 1917; Fulks 1962). The recent theoretical work of Davies-Jones (1984) and Rotunno and Klemp (1985) on the origin of midlevel rotation has turned the focus toward the low-level wind profile, as seen first by van Everdingen (1925) and more recently in a number of studies (e.g., Rasmussen and Wilhelmson 1983; Patrick and Keck 1987; Schaefer and Livingston 1988). While the importance of the low-level winds in developing supercells has been shown theoretically and with numerical models, it appears that the importance of the midtropospheric winds in determining the low-level structure of supercells rests in their ability to redistribute precipitation in the vicinity of the storm. Thus, the observational evidence of strong upper-level winds associated with tornadic events may have been, in some sense, serendipitous. Based on our results, the role of the midtropospheric wind shear appears to be indirect.[4] Whereas Wegener (1917) and Fulks (1962) invoked tilting of horizontal vorticity downward from near the top of thunderstorms to produce low-level vertical vorticity, the simulations indicate that the primary effect of changing midtropospheric shear is to alter the magnitude of the midtropospheric winds. By changing the storm motion and the location of precipitation and the cooling that results from the associated evaporation, the dynamics of the low-level mesocyclone are altered.

Acknowledgments. Some of this work was done while one of the authors (HEB) held a National Research Council–NOAA Research Associateship. The computer simulations were carried out on the CRAY-2 at the National Center for Supercomputer Applications (NCSA), and software developed at NCSA was used in the analysis of the data. The simulations were supported, in part, by NSF Grants ATM-87-00778 and ATM 92-14098. We thank Messrs. Michael Magsig and Donald Burgess for their observations from the WSR-88D radar at Twin Lakes, Oklahoma, of rotation in the 26 April 1991 Red Rock, Oklahoma, storm. We thank the operational forecasters at the National Severe Storms Forecast Center and at the 1993 Atmospheric Environment Service (Canada) Summer Severe Weather Workshop for their encouragement and anecdotal observations supporting the conceptual model. Discussions with Robert Davies-Jones and Erik Rasmussen helped us clarify our thoughts.

[4] We note also that none of the observational studies have considered tornadic versus nontornadic *supercells,* which would be the ideal comparison in order to test the conceptual model against observations. Development of a large enough dataset of environmental conditions to provide statistically meaningful information about nontornadic supercells awaits the continued deployment and operation of the WSR-88D radar network, as well as thorough verification of storm behavior.

REFERENCES

Brooks, H. E., C. A. Doswell III, and R. Davies-Jones, 1993: Environmental helicity and the maintenance and evolution of low-level mesocyclones. *The Tornado: Its Structure, Dynamics, Prediction, and Hazards, Geophys. Monogr.,* C. Church, Ed., No. 79, Amer. Geophys. Union, 97–104.

Burgess, D. W., and L. R. Lemon, 1990: Severe thunderstorm detection by radar. *Radar in Meteorology,* D. Atlas, Ed., Amer. Meteor. Soc., 619–647.

——, and M. A. Magsig, 1993: Radar evolution of the Red Rock, Oklahoma supercell of April 26, 1991. Preprints, *17th Conf. on Severe Local Storms,* St. Louis, MO, Amer. Meteor. Soc., in press.

Davies-Jones, R., 1984: Streamwise vorticity: The origin of updraft rotation in supercell storms. *J. Atmos. Sci.,* **41,** 2991–3006.

——, and H. Brooks, 1993: Mesocyclogenesis from a theoretical perspective. *The Tornado: Its Structure, Dynamics, Prediction, and Hazards, Geophys. Monogr.,* C. Church, Ed., No. 79, Amer. Geophys. Union, 105–114.

——, D. Burgess, and M. Foster, 1990: Test of helicity as a tornado forecast parameter. Preprints, *16th Conf. on Severe Local Storms,* Kananaskis Park, Alberta, Canada, Amer. Meteor Soc., 588–592.

Doswell, C. A., III, 1985: The operational meteorology of convective weather. Volume II: Storm scale analysis. NOAA Tech. Memo. ERL ESG-15, 240 pp. [Available from the author at NSSL, 1313 Halley Circle, Norman, OK 73069.]

Droegemeier, K. K., S. M. Lazarus, and R. Davies-Jones, 1993: The influence of helicity on numerically simulated convective storms. *Mon. Wea. Rev.,* **121,** 2005–2029.

Fawbush, E. J., and R. C. Miller, 1952: A mean sounding representative of the tornadic airmass environment. *Bull. Amer. Meteor. Soc.,* **33,** 303–307.

——, and R. C. Miller, 1954: The types of airmasses in which North American tornadoes form. *Bull. Amer. Meteor. Soc.,* **35,** 154–165.

——, ——, and L. G. Starrett, 1951: An empirical method for forecasting tornado development. *Bull. Amer. Meteor. Soc.,* **32,** 1–9.

Fujita, T. T., D. L. Bradbury, and C. F. Van Thullenar, 1970: Palm Sunday tornadoes of April 11, 1965. *Mon. Wea. Rev.,* **98,** 29–69.

Fulks, J. R., 1962: On the mechanics of the tornado. National Severe Storms Project Report No. 4, 33 pp.

Klemp, J. B., and R. B. Wilhelmson, 1978: The simulation of three-dimensional convective storm dynamics. *J. Atmos. Sci.,* **35,** 1070–1096.

Lilly, D. K., 1986: The structure, energetics, and propagation of rotating convective storms. Part II: Helicity and storm stabilization. *J. Atmos. Sci.,* **43,** 126–140.

Marwitz, J. D., 1972: The structure and motion of severe hailstorms. Part I: Supercell storms. *J. Appl. Meteor.,* **11,** 166–179.

Moller, A. R., C. A. Doswell III, and R. Pryzybylinski, 1990: High-precipitation supercells: A conceptual model and documentation. Preprints, *16th Conf. on Severe Local Storms,* Kananaskis Park, Alberta, Canada, Amer. Meteor. Soc., 52–57.

Patrick, D., and A. J. Keck, 1987: The importance of the lower level windshear profile in tornado/non-tornado discrimination. *Proc. Symp. Mesoscale Analysis and Forecasting,* ESA, 393–397.

Rasmussen, E. N., and R. B. Wilhelmson, 1983: Relationships between storm characteristics and 1200 GMT hodographs, low level shear, and stability. Preprints, *13th Conf. on Severe Local Storms,* Tulsa, OK, Amer. Meteor. Soc., J5–J8.

Rotunno, R., and J. B. Klemp, 1985: On the rotation and propagation of simulated supercell thunderstorms. *J. Atmos. Sci.,* **42,** 271–292.

Schaefer, J. T., and R. L. Livingston, 1988: The typical structure of tornado proximity soundings. *J. Geophys. Res.,* **93,** 5351–5364.

Shuman, F. G., and L. P. Carstensen, 1952: A preliminary tornado forecasting system for Kansas and Nebraska. *Mon. Wea. Rev.,* **80,** 233–240.

van Everdingen, E., 1925: The cyclone-like whirlwinds of August 10, 1925: *Proc., Royal Academy of Amsterdam Section of the Science,* **25,** 871–889.

Wegener, A., 1917: *Wind- und Wasserhosen in Europa.* Friedrich Vieweg und Sohn, 301 pp. (In German.)

Weisman, M. L., and J. B. Klemp, 1984: The structure and classification of numerically simulated convective storms in directionally varying wind shears. *Mon. Wea. Rev.,* **112,** 2479–2498.

——, and ——, 1982: The dependence of numerically simulated convective storms on vertical wind shear and buoyancy. *Mon. Wea. Rev.,* **110,** 504–520.

Wicker, L. J., and R. B. Wilhelmson, 1990: Numerical simulation of tornado-like vortex in a high resolution three dimensional cloud model. Preprints, *16th Conf. on Severe Local Storms,* Kananaskis Park, Alberta, Canada, Amer. Meteor Soc., 263–268.

Wilhelmson, R. B., and J. B. Klemp, 1981: A three-dimensional numerical simulation of splitting severe storms on 3 April 1964. *J. Atmos. Sci.,* **35,** 1037–1063.

——, and C. S. Chen, 1982: A simulation of the development of successive cells along a cold outflow boundary. *J. Atmos. Sci.,* **39,** 1466–1483.